Electronic Supplementary Information

New Journal of Chemistry

Shell Decoration of Hydrothermally Obtained Colloidal Carbon Spheres with Base Metal Nanoparticles

Jacco Hoekstra,[a] Andrew M. Beale,[b,c,d] Fouad Soulimani,[b] Marjan Versluijs-Helder,[b] John W. Geus,[a] Leonardus W. Jenneskens[a]

[a] Organic Chemistry and Catalysis, Debye Institute for Nanomaterials Science, Utrecht University, Universiteitsweg 99, 3584 CA Utrecht, the Netherlands

[b] Inorganic Chemistry and Catalysis, Debye Institute for Nanomaterials Science, Utrecht University, Universiteitsweg 99, 3584 CA Utrecht, the Netherlands

[c] UK Catalysis Hub, Research Complex at Harwell, Rutherford Appleton laboratory, Harwell, Didcot, Oxfordshire, OX11 oFA, UK

[d] Department of Chemistry, University College London, 20 Gordon Street, London WC1H, oAJ, UK

Contents

Fig. S1. FT-IR spectrum of the CCS after work-up.

Fig. S2. Ellingham diagrams of the carbothermal reduction of the base metal oxides: copper (a), nickel (b), cobalt (c) and iron (d).

Fig. S3. The original CCS (left) and the CCS after pyrolysis at T = 800 °C (right) in a biphasic system of water/hexane.

Fig S4. Deconvolution results of the first-order (a) and second-order (b) Raman spectrum of the CCS after pyrolysis at T = 800 °C (* = N_2).

Fig. S5. TGA (air) of CCS-supported base metal nanoparticles after pyrolysis at T = 800 °C.

Fig. S6. Raman spectra of the CCS loaded with copper (a), nickel (b) and cobalt (c) after pyrolysis at T = 800 °C (* = N_2).

Table S1. Elemental analysis and atomic ratios of sucrose and CCS samples.

Table S2. Deconvolution results of the Raman spectra of the CCS samples loaded with base metal nanoparticles after pyrolysis at T = 800 °C.

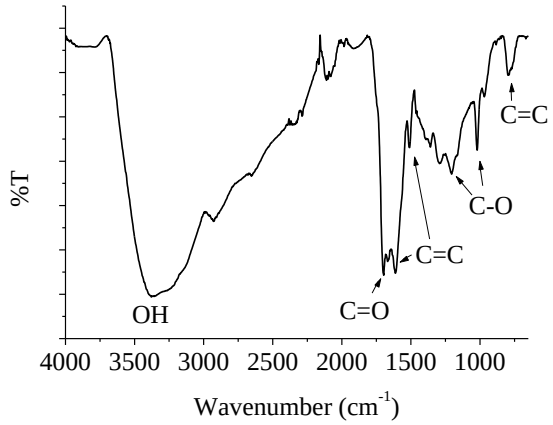

Fig. S1. FT-IR spectrum of the CCS after work-up.

The FT-IR spectrum resembles that of the FT-IR spectrum obtained from the HTC of glucose (see ref. 3). Various hydrophilic oxygen containing functional groups are indicated in the FT-IR spectrum.

The FT-IR spectrum shows O-H stretch vibrations (3340 cm^{-1}), carbonyl stretch vibrations (1700 cm^{-1}), C-O stretch vibrations (1204 cm^{-1} and 1020 cm^{-1}), C=C stretch vibrations at 1611 cm^{-1}, 1509 cm^{-1} and 789 cm^{-1} (aromatic core).[63]

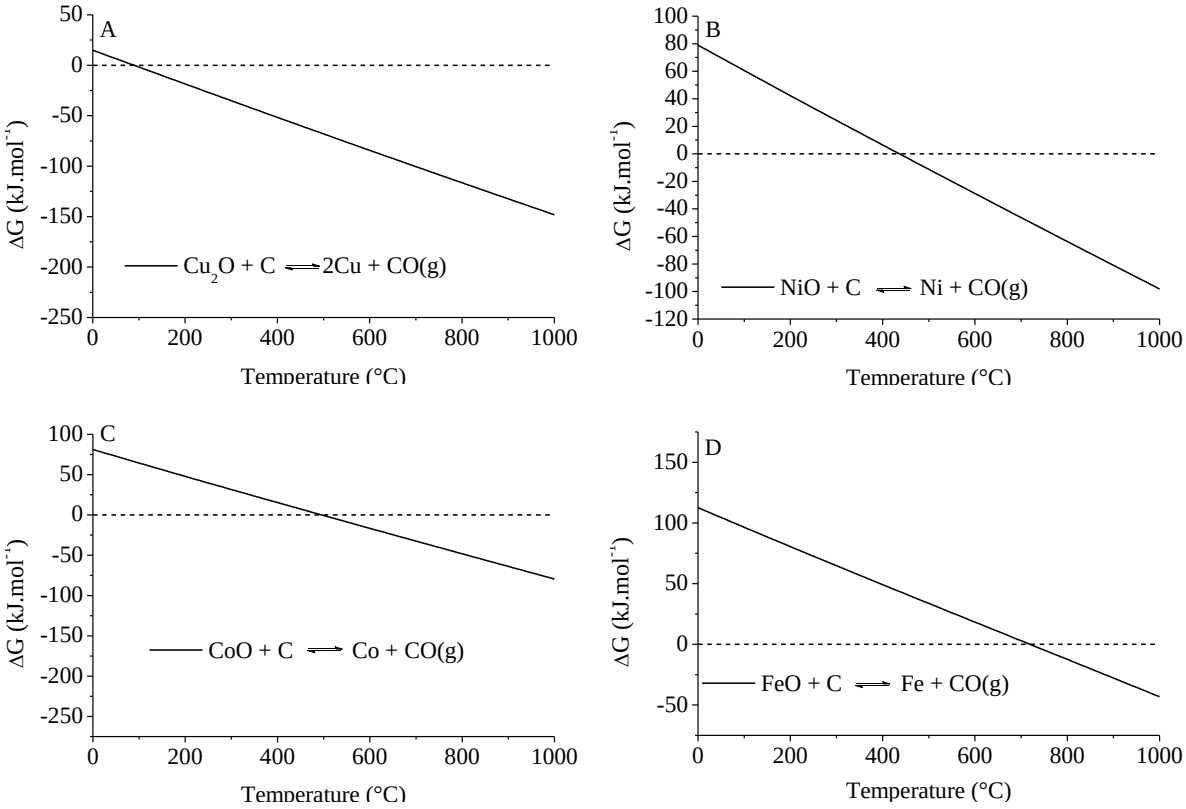

Fig. S2. Ellingham diagrams of the carbothermal reduction of the base metal oxides: copper (a), nickel (b), cobalt (c) and iron (d).

In previous work from the pyrolysis of microcrystalline cellulose spheres loaded with base metal salts[27] we found that pyrolysis of these loaded bodies resulted in the formation of amorphous carbonaceous bodies with base metal oxide nanoparticles dispersed in them. At increasing temperature the base metal oxide nanoparticles reduced stepwise, *i.e.* CuO → Cu_2O → Cu, NiO → Ni, Co_3O_4 → CoO → Co and Fe_3O_4 → FeO → Fe. The final reduction steps are displayed in the Ellingham diagrams, taking into account the Boudouard equilibrium ($C + CO_2 \leftrightarrows 2CO$), which lies at the CO side at elevated temperatures (T > 700 °C).[40,41] The Ellingham diagrams show that carbothermal reduction of the respective base metal oxides is feasible at the temperature of pyrolysis employed (T = 800 °C).

Fig. S3. The original CCS (left) and the CCS after pyrolysis at T = 800 °C (right) in a biphasic system of water/hexane.

The original CCS are hydrophilic due to the oxygen-containing functionalities on their surface. Therefore in a water/hexane biphasic system the CCS are distributed in the aqueous phase. Due to the pyrolysis the carbonaceous material becomes hydrophobic and ends up in the hexane layer.

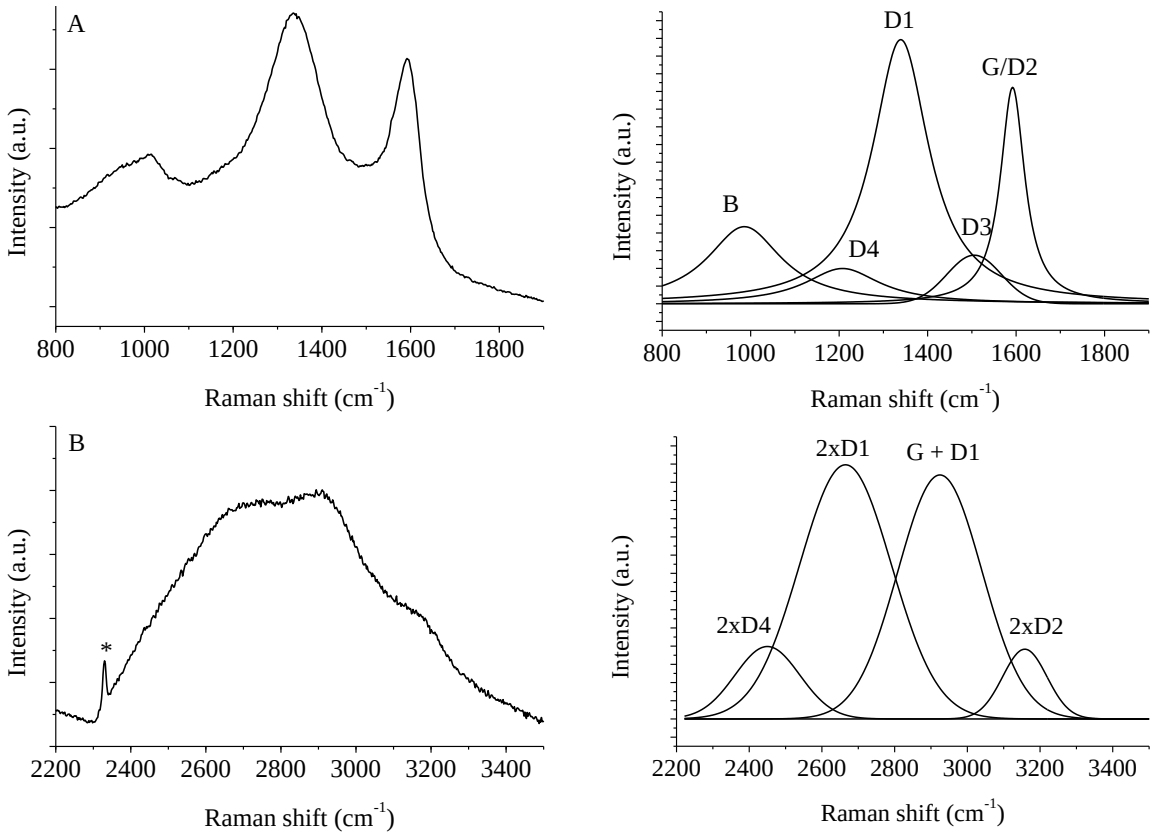

Fig. S4. Deconvolution results of the first-order (a) and second-order (b) Raman spectrum of the CCS after pyrolysis at T = 800 °C (* = N_2). Note the additional background peak around 1000 cm^{-1}, which represents an artefact of the experimental setup. It was taken into consideration with the deconvolution procedure, denoted as B (Table S2).

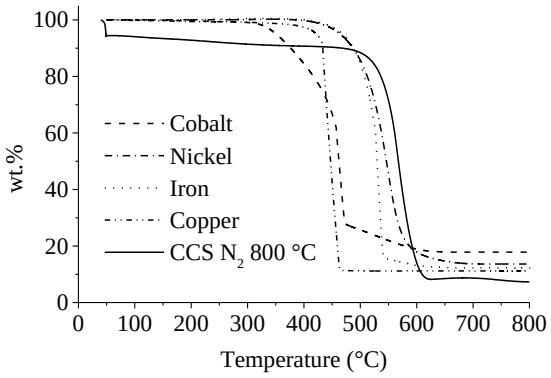

Fig. S5. TGA (air) of CCS-supported base metal nanoparticles after pyrolysis at T = 800 °C.

The ash residue of the CCS after pyrolysis in air (T = 800 °C.) was 7.2 wt.%. It was anticipated that the base metals were converted to their most stable oxidic forms, *viz.*, CuO, NiO, Co_3O_4 and Fe_3O_4. The base metal loading, after correction for the ash residue, were calculated accordingly: Cu 3.5 wt.%, Ni 5,1 wt.%, Co 1.5 wt.% and Fe 1.2 wt.%.

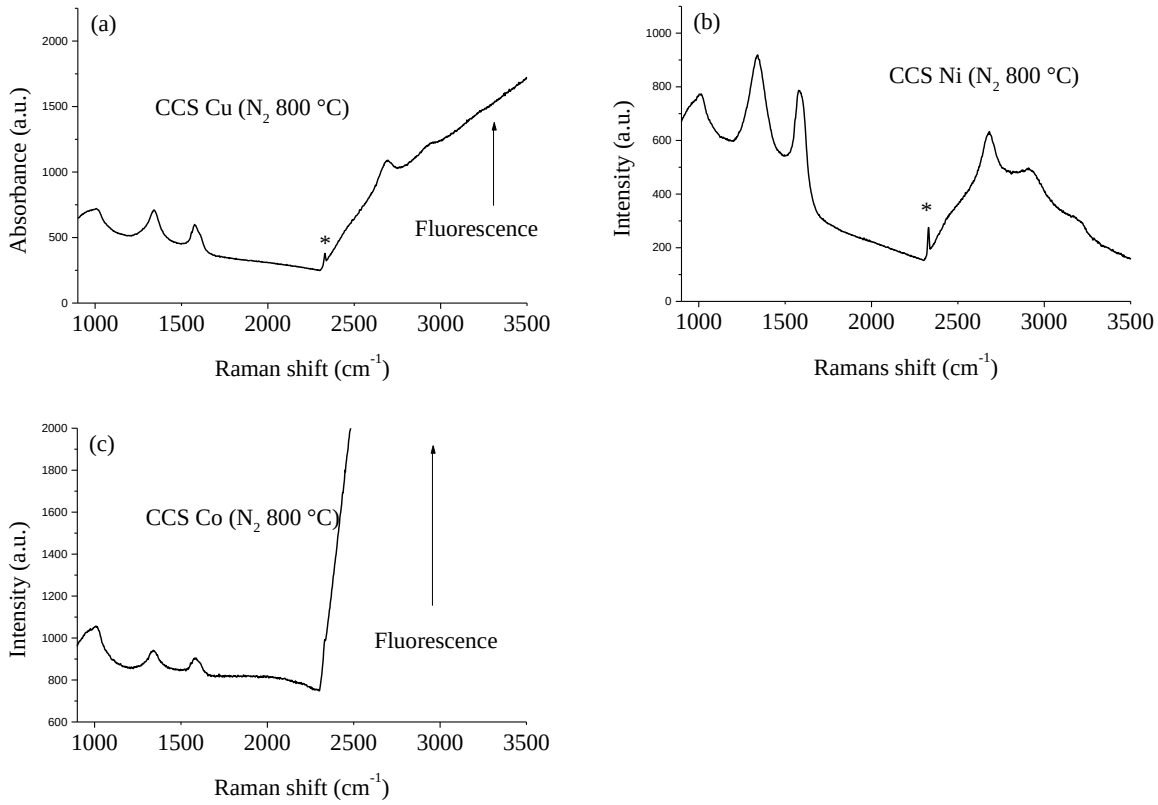

Fig. S6. Raman spectra of the CCS loaded with copper (a), nickel (b) and cobalt (c) after pyrolysis at T = 800 °C (* = N_2). Due to the occurrence of fluorescence the 2nd-order part of the Raman spectrum of the sample containing cobalt obtained after pyrolysis at T = 800 °C could not be deconvoluted (See also Table S2).

Table S1. Elemental analysis and atomic ratios of sucrose and CCS samples.

Sample	C (wt.%)	H (wt.%)	O (wt.%)	H/C	O/C
Sucrose	42.11	6.43	51.46	1.83	0.92
CCS	59.55	5.98	33.21	1.20	0.42
CCS N_2 800 °C	82.74	5.34	10.21	0.77	0.10

Elemental analysis shows an increase in the amount of carbon at the expense of hydrogen and oxygen when the sucrose is hydrothermally treated. The oxygen content is still reasonably high, which confirms that oxygen functionalities are present (*cf.* also Figure S1).

After pyrolysis at T = 800 °C of the CCS elemental analysis shows that the wt.% of carbon increases with respect to wt.% of hydrogen and, particularly, wt.% of oxygen; organic functional groups are lost. Notwithstanding, a significant amount of oxygen remains incorporated even after treatment at T = 800 °C.[42,43] This indicates, that primarily the oxygen functionalities of the shell, *viz.* near the perimeter, are lost while the more stable bridged oxygen functionalities of the furan derivatives in the original core survive.

Table S2. Deconvolution results of the Raman spectra of the CCS samples loaded with base metal nanoparticles after pyrolysis at T = 800 °C.

Sample	Position (cm^{-1})	FWHM (cm^{-1})
CCS, N_2 800 °C		
B	986	204
D4	1208	206
D1	1340	156
D3	1506	144
G/D2	1592	66
2×D4	2450	210
2×D1	2664	296
G+D1	2924	272
2×D2	3158	142
CCS, Cu N_2 800 °C		
B	984	192
D4	1208	200
D1	1340	154
D3	1506	148
G/D2	1594	64
2×D4	2450	158
2×D1	2670	302
G+D1	2930	248
2×D2	3160	166
CCS, Ni N_2 800 °C		
B	994	184
D4	1170	202
D1	1340	136
D3	1506	152
G/D2	1588	66
2×D4	2490	214
2×D1	2674	172
G+D1	2906	292
2×D2	3168	138
CCS, Co N_2 800 °C		
B	982	176
D1	1340	92
D3	1500	222
G	1580	44
D2	1610	26
CCS, Fe N_2 800 °C		
B	984	186
D4	1258	256
D1	1342	90
D3	1500	174
G	1580	52
D2	1610	34
2×D4	2548	278
2×D1	2684	106
G+D1	2884	316
2×D2	3182	150